Parameter calibration and application of fracture models to high-performance steel seismic dampers

Conference Paper · September 2014

CITATIONS
0

READS
43

4 authors:

G. Vasdravellis
Heriot-Watt University
48 PUBLICATIONS **447** CITATIONS
SEE PROFILE

Theodore L. Karavasilis
University of Patras
93 PUBLICATIONS **1,224** CITATIONS
SEE PROFILE

Brian Uy
The University of Sydney
64 PUBLICATIONS **238** CITATIONS
SEE PROFILE

Vasileios Kamperidis
Abertay University
6 PUBLICATIONS **11** CITATIONS
SEE PROFILE

PARAMETER CALIBRATION AND APPLICATION OF FRACTURE MODELS TO HIGH-PERFORMANCE STEEL SEISMIC DAMPERS

George Vasdravellis[a], Theodore L. Karavasilis[b], Brian Uy[c], Vasilis Kamperidis[b]

[a] Heriot-Watt University, Institute for Infrastructure and Environment, UK
g.vasdravellis@hw.ac.uk
[b] University of Warwick, School of Engineering, UK
t.l.karavsilis@warwick.ac.uk; v.kamperidis@warwick.ac.uk
[c] University of New South Wales, Centre for Infrastructure Engineering and Safety, Australia
b.uy@unsw.edu.au

1 INTRODUCTION

Steel cylindrical pins with hourglass-shape bending parts (called web hourglass pins – WHPs) have been recently used by the authors [1] as the energy dissipation system of a steel post-tensioned (PT) beam-column connection for self-centering moment-resisting frames (SC-MRFs). Pilot tests on WHPs showed their superior energy dissipation and fracture capacity [1]. However, more work is needed to assess the hysteretic behavior and low-cycle fatigue performance of WHPs for high performance steel materials such as high strength steel (HSS) and stainless steel (SS). There is limited experience on the low-cycle fatigue and fracture capacity of SS for seismic applications. SS grades are divided into three categories: austenitic, ferritic, and duplex. Austenitic is the most common type of SS. Duplex SS (referred to herein as SSD) is at least twice stronger than the common austenitic grades and highly resistant to corrosion cracking.

This paper presents the application of two micromechanics-based models for ductile fracture prediction in metals, i.e. the Void Growth Model (VGM) and the Stress Modified Critical Strain Model (SMCS). First, the critical parameters of the two models are identified using tensile tests on circumferentially-notched specimens (CNS) and complementary numerical analysis based on the finite element method (FEM). The critical parameters of the VGM and SMCS are then used to predict fracture in WHPs made of HSS grade M1020, SS grade 304 (SS304), and SSD. Finally, the ability of the cyclic VGM (or CVGM) to predict ductile fracture under cyclic loading conditions is evaluated using the results of several cyclic tests on WHPs made of HSS and SS304.

2 THE VGM AND SMCS MODELS FOR DUCTILE FRACTURE PREDICTION

The VGM and SMCS model are based on prior theoretical and experimental research on ductile crack initiation in metals, see for example Hancock and Mackenzie [2], Panontin and Sheppard [3]. These studies have shown that ductile fracture is associated with two key quantities: the equivalent plastic strain (PEEQ) and the stress triaxiality, defined as the ratio of the mean stress, σ_m, to the vonMises stress, σ_e. The VGM is based on the findings of Rice and Tracey [4] and was successfully applied to predict ductile failure initiation in seven steel grades by Kanvinde and Deierlein [5]. According to this model, ductile fracture initiates when a quantity named Void Growth Index (*VGI*) reaches a critical value. The *VGI* is defined as:

$$VGI = \int_0^{\varepsilon_{cr}^p} \exp\left(-1.5\frac{\sigma_m}{\sigma_e}\right) d\varepsilon_p \geq VGI_{cr} \quad (1)$$

where ε_{cr}^p is the PEEQ at the time of ductile crack initiation. Calculation of the *VGI* requires integration of the exponential expression of triaxiality with respect to the PEEQ over the loading history until fracture. The SMCS model is based on the research of Hancock and Mackenzie [2] and assumes that triaxiality is practically constant during the loading. It is computationally less

demanding than the VGM as it does not require integration and calculates ε_{cr}^{p} based on instantaneous values of the triaxiality at the time of crack initiation according to:

$$\varepsilon_{cr}^{p} = \alpha \exp\left(-1.5\frac{\sigma_m}{\sigma_e}\right) \quad (2)$$

where α is the toughness index that is considered a material constant to be determined. The calibration of the parameters VGI_{cr} and α of the VGM and SMCS model requires tensile tests on CNS and complementary FEM analyses.

3 PARAMETER CALIBRATION OF THE VGM AND SMCS MODELS FOR HIGH-STRENGTH AND STAINLESS STEEL

Twenty-seven tensile tests on CNS were conducted, i.e. nine for each of the M1020, SS304 and SSD. The geometry of the CNS is shown in *Fig. 1a*. Three different radii were used to create the notch at the central region of the CNS, i.e. R= 2, 3, and 4.5 mm and three specimens were tested for each radius. The notch creates a triaxial stress state at the CNS central region and the level of triaxiality depends on R, i.e. smaller R creates higher triaxiality. The CNS were loaded in axial tension and a typical force – displacement curve up to fracture is shown in *Fig. 1c*.
The CNS tests were simulated using FEM in the commercial software Abaqus [6]. An axisymmetric model was created taking into account the symmetry of the specimens as shown in *Fig. 1b*. Following the recommendations of Kanvinde and Deierlein [5], an element size of 0.2 mm was created at the notch region to accurately capture the stress and strain gradients around the fracture initiation location. The results of the tensile tests were used to define the true stress – plastic strain laws of the three materials as required for FEM simulation. *Fig. 1c* compares the experimental and numerical force – displacement curves for a SS304 CNS with R= 3 mm and demonstrates a good agreement up to the fracture. Similar agreement was achieved for all the CNS tests.
The stress and strain output from FEM analyses are used to determine the parameters VGI_{cr} and α. VGI_{cr} is determined by numerically integrating *Eq. 1* at the center of the CNS ("Node 1" in *Fig. 1b*) where fracture initiates. α is calculated from *Eq. 2* and the instantaneous values of stress and strain in the FEM model at the time of fracture at the CNS center. *Table 1* summarizes the values of VGI_{cr} and α which should be considered as reliable considering their relatively small standard deviation values. The largest VGI_{cr} and α values (3.37 and 3.53) correspond to the SS304 material, while the smallest ones (2.17 and 2.58) to the M1020 material. These results are consistent with the ductility of each material, i.e. a higher VGI_{cr} or α corresponds to a more ductile material, as demonstrated by the uniaxial tensile tests and reported in Vasdravellis et al. [7].

3.1 VGM application to WHPs

The calibrated VGM was used to study the fracture behavior of WHPs under monotonic loading. Three-dimensional FEM models of the WHPs and the supporting plates were constructed as shown in *Fig. 2*. The FEM model consists of linear hexahedral elements with reduced integration and makes use of the symmetrical geometry. Contact interactions between the supporting plates and the WHPs were applied. The WHP mesh is more refined than the mesh of the supporting plates with maximum refinement within the bending parts of the WHPs (see *Fig. 2a*). In the FEM model of the WHPs the mesh of the bending parts consisted of elements with an approximate size of 0.5 – 1 mm (*Fig. 2b*). *Fig. 2c* shows a representative force – displacement comparison indicating that the numerical model is in good agreement with the tests.
Fig. 3 shows the deformed shape of a WHP at 25 mm imposed displacement and a contour plot of the PEEQ distribution. The maximum PEEQ is located at the center of the half – bending part of the WHP (Section 2), while the maximum triaxiality is located at the end of the bending part near the web (Section 1). During the cyclic tests, fracture typically initiated at the point of maximum triaxiality, although fracture at the location of maximum PEEQ was also observed.

Fig. 4 plots the variation of the *VGI* across the length of the half – bending – parts of the WHPs and *Table 2* reports the corresponding values for a monotonically imposed displacement of 25 mm. The *VGI* is computed at the top, most-stressed, elements. The maximum *VGI* is located at Section 1 for SS304 and SSD and at Section 2 for M1020 material. These results are consistent with the fracture initiation locations during the cyclic tests [7]. At the center of the WHP, *VGI* has very small values. The values of *VGI* under this excessive imposed displacement are much lower than VGI_{cr} (see *Table 1*), indicating very low likelihood of fracture under monotonic loading.

Table 1. Summary of the CNS tests for the VGI_{cr} and α_{SMCS} parameters calibration

Material	Notch size	VGI_{cr}	α
HSS	*R*= 2	2.29	2.96
	R= 3	2.14	2.50
	R= 4	2.06	2.30
	Mean	*2.17*	*2.58*
	St. Dev.	*0.11*	*0.34*
SS304	*R*= 2	3.74	3.70
	R= 3	3.31	3.92
	R= 4	3.04	2. 7
	Mean	*3.37*	*3.53*
	St. Dev.	*0.35*	*0.49*
SSD	*R*= 2	2.88	2.67
	R= 3	3.02	2.64
	R= 4	2.70	2.63
	Mean	*2.87*	*2.65*
	St. Dev.	*0.16*	*0.02*

Table 2. VGI values at three sections along the WHP

No axial restraint	Center	Section 2	Section 1
HSS	0.1	**0.71**	0.65
SS304	0.31	0.5	**0.56**
SSD	0.23	0.55	**0.62**
Axial restraint	**Center**	**Section 2**	**Section 1**
HSS	**0.91**	0.66	0.42
SS304	**0.55**	0.53	**0.55**
SSD	**0.81**	0.56	0.42
Note: Maximum values are in bold			

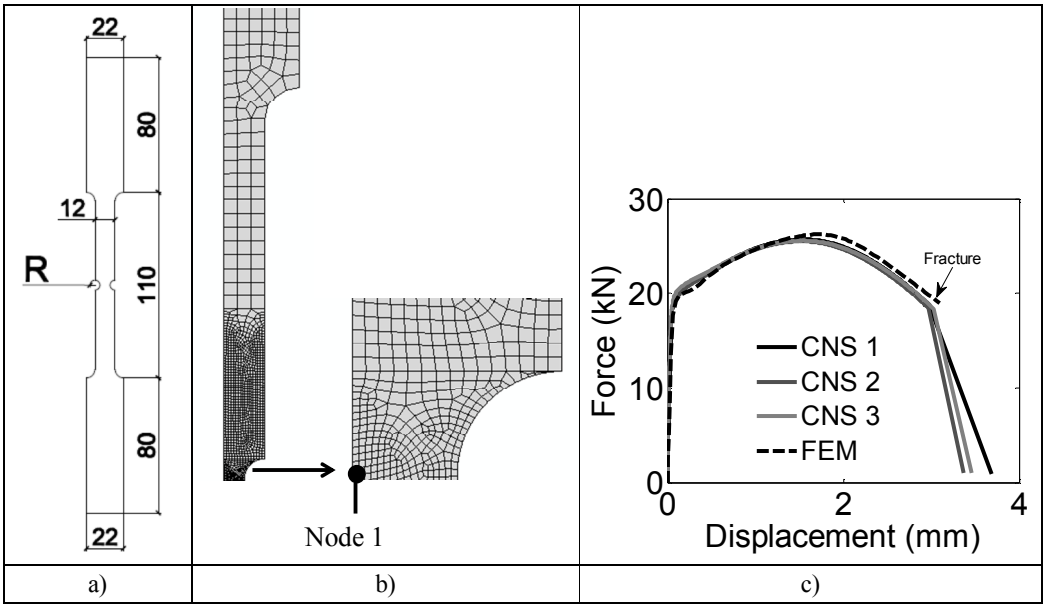

Fig. 1. a) CNS geometry; b) axisymmetric FEM model of a CNS (half specimen); and c) experimental – FEM comparison for the CNS tests.

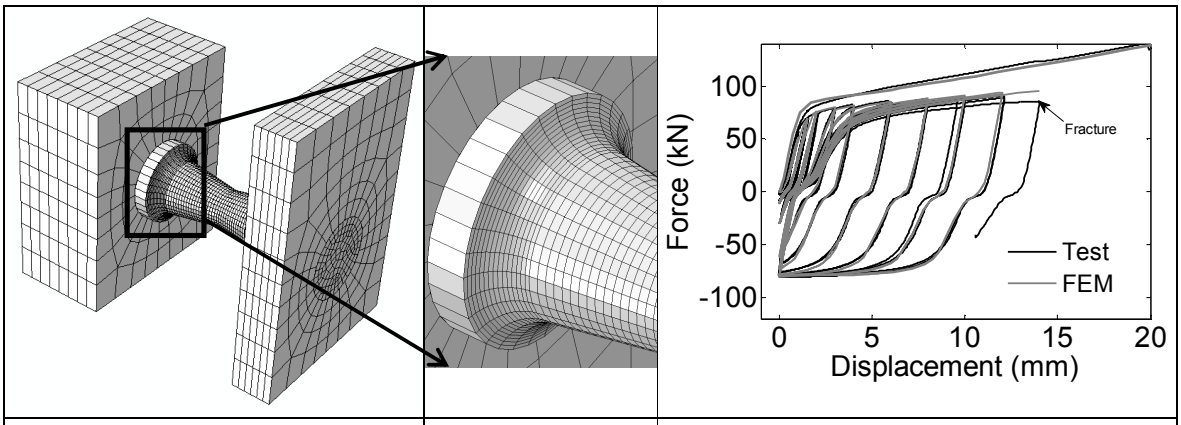

Fig. 2. a) WHP FEM model; b) mesh refinement; and c) experimental – FEM comparison for the HSS-WHP1 under the AISC loading protocol.

3.2 Effect of axial restrain on VGM distribution

During the cyclic tests, the WHPs have been slightly translated with respect to the web. In a real building application, the WHPs can be axially restrained to eliminate this translation by threading part of the external parts and using a set of washers to secure them against axial movement. FEM simulations show that axial restraint results in different PEEQ distribution along the bending parts. The maximum PEEQ is located at the center, near the section with diameter D_i, as shown in *Fig. 3b*. The *VGI* distribution of WHPs with axial restrain is plotted in *Fig. 4* with grey lines and the corresponding values are reported in *Table 2*. The maximum *VGI* is located at the center of the bending part, which coincides with the location of maximum PEEQ, indicating this section as the location of fracture initiation in an axially-restrained WHP. The maximum *VGI* values are larger than the maximum values in the no axial restraint case; they are still though considerably smaller than the VGI_{cr}, having values between 0.8 - 0.9 at an excessive displacement of 25 mm.

4 APPLICATION OF THE CYCLIC VGM

To predict fracture initiation in the WHPs under cyclic loading, the CVGM proposed by Kanvinde and Deierlein [8] was used. The model follows the same assumptions with the VGM but is modified to account for positive and negative triaxiality that develops during cyclic loading. The model is intended for seismic applications, where fracture in metals typically occurs due to Ultra Low Cycle Fatigue (ULCF). The model assumes that only tensile cycles can cause fracture in the material. Fracture under cyclic loading occurs when a value called VGI_{cyclic} exceeds the critical value $VGI_{cyclic}^{critical}$. The VGI_{cyclic} is calculated from stress and strain histories obtained from FEM analyses, while the $VGI_{cyclic}^{critical}$ is calculated as a degraded function of the monotonic VGI_{cr}:

$$VGI_{cyclic}^{critical} = VGI_{cr}\exp(-\lambda\varepsilon_p^{acc}) \quad (3)$$

where ε_p^{acc} is a damage variable defined as the PEEQ that has accumulated up to the beginning of each "tensile" cycle [8], and λ is the rate of degradation of the monotonic VGI_{cr}. A higher value of λ results in a faster degradation. The combined isotropic – kinematic hardening material model of Abaqus was calibrated iteratively and used in FEM analysis. A representative hysteresis comparison is shown in *Fig. 3c* and reveals the ability of the FEM model to simulate the experimental hysteresis prior to fracture.

Fig. 5 shows the VGI_{cyclic} - $VGI_{cyclic}^{critical}$ plot for the random loading protocol. The VGI_{cyclic} increases and decreases based on the sign of triaxiality, while $VGI_{cyclic}^{critical}$ is a step-wise descending function as

a result of the damage variable definition. Ductile fracture initiation is predicted to occur at the intersection of the two lines. The quantities VGI_{cyclic} and $VGI_{\text{cyclic}}^{\text{critical}}$ were calculated using the stress and strain histories of the FEM simulation. *Fig. 5* plots the evolution of VGI_{cyclic} and $VGI_{\text{cyclic}}^{\text{critical}}$ in Sections 1 and 2. While the fracture of the HSS-WHP1 specimen started from Section 1, which is the location of maximum triaxiality, the CVGM criterion in the FEM simulation is satisfied first at Section 2 which is the location of maximum PEEQ. Although the triaxiality in Section 1 is higher than that that at Section 2, the demands due to the PEEQ concentration at Section 2 result in a more accelerated satisfaction of the CVGM criterion. Similar results were obtained for the other three cyclic loading histories, i.e. the CVGM criterion is always satisfied faster at Section 2.

Compared with the experiments, the model predicts fracture at a different location than that observed in the tests, although the predictions are in relatively good agreement with the experimental values. Fracture at Section 1 is predicted to occur several cycles after the fracture at Section 2 and does not agree with the experimental results for the specific value of λ.

This tentative application of the CVGM with λ values taken from the literature indicates that the model may not give accurate results for the specific application. Possible reasons for that may be: a) the model may need further modification to accurately predict fracture due to ULCF in steel components where the locations of maximum PEEQ and maximum triaxiality are different as in the case of WHPs; and b) the CVGM was based on the results of tensile tests on CNS where triaxiality at fracture has high values (0.7 – 1.6), while the maximum triaxiality in the WHPs was in the range 0.4 – 0.5. The CVGM may need further modification and calibration for relatively low values of triaxiality observed in the WHPs.

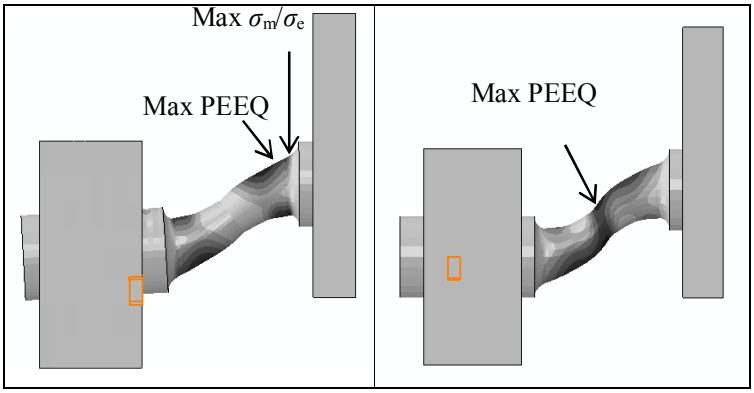

Fig. 3. WHP at 25 mm imposed displacement and PEEQ contour plot: a) no axial restraint; b) axial restraint.

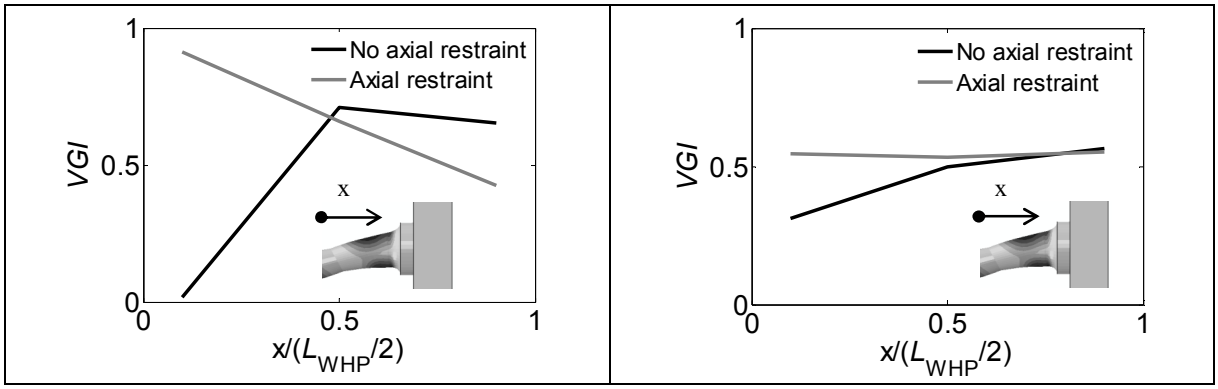

Fig. 4. VGI distribution along the length of WHPs under monotonic loading: a) HSS-WHP1; b) SS304-WHP1.

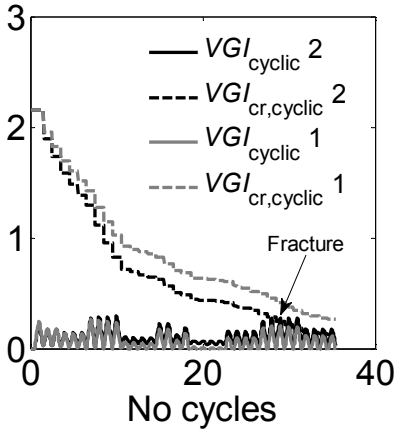

Fig. 5. Prediction of fracture in specimen HSS-WHP1 under random cyclic loading according to CVGM

5 CONCLUSIONS

- The void growth model (VGM) and the stress-modified critical strain (SMCS) model used to predict fracture in metals were calibrated for the HSS, SS and SSD and their parameters (critical void growth index VGI_{cr} and toughness index α) are provided. The values of these parameters are consistent with the ductility of the materials.
- Application of the VGM to the monotonic tests of the WHPs resulted in *VGI* values considerably lower than the VGI_{cr} at the critical locations, confirming the very low likelihood of fracture under monotonic loading. Axial restraint imposed on WHPs changes the critical location of potential fracture.
- Application of the cyclic VGM, with λ (rate of degradation of the monotonic VGI_{cr}) values taken from literature, to four cyclic WHP tests predicted fracture at a different location than that observed in the tests. Possible reasons for this discrepancy were discussed.
- WHPs made of HSS, SS and SSD are reliable devices that can be safely used as seismic energy-dissipative fuses in beam-column connections and braces with the goal of realizing a very easy-to-repair structural design concept.

REFERENCES

[1] Vasdravellis, G., Karavasilis, T.L., and Uy, B. (2013a). "Large-scale experimental validation of steel post-tensioned connections with web hourglass pins". J. Struct. Eng. 139(6), 1033-1042.

[2] Hancock, J. W., Mackenzie, A. C. (1976). "On the mechanics of ductile failure in high-strength steel subjected to multi-axial stress states." J. Mech. Phys. Solids, 24(3), 147–169.

[3] Panontin, T. L., and Sheppard, S. D. (1995). "The relationship between constraint and ductile fracture initiation as defined by micromechanical analyses." *Fracture mechanics: 26th Volume*, *ASTM STP 1256*, ASTM, West Conshohoken, Pa., 54–85.

[4] Rice, J.R. and Tracey, D.M. (1969). "On the ductile enlargement of voids in triaxial stress fields". *J. Mech. Phys. Solids*, 17(3), 201-217.

[5] Kanvinde, A. M., and Deierlein, G. G. (2006). "The void growth model and the stress modified critical strain model to predict ductile fracture in structural steels." J. Struct. Eng., 132(12), 1907-1918.

[6] Abaqus user's manual

[7] Vasdravellis G., Karavasilis T.L.,Uy B. (2014). "Design rules, experimental evaluation and fracture models of high-strength and stainless-steel hourglass shape energy dissipation devices". Journal of Structural Engineering (ASCE). Accepted – in press

[8] Kanvinde, A. M., and Deierlein, G. G. (2007). "Cyclic void growth model to assess ductile fracture initiation in structural steels due to ultra-low cycle fatigue." J. Eng Mech., 133(6), 701-712.

PARAMETER CALIBRATION AND APPLICATION OF FRACTURE MODELS TO HIGH-PERFORMANCE STEEL SEISMIC DAMPERS

George Vasdravellis[a], Theodore L. Karavasilis[b], Brian Uy[c], Vasilis Kamperidis[b]

[a] Heriot-Watt University, Institute for Infrastructure and Environment, UK
g.vasdravellis@hw.ac.uk
[b] University of Warwick, School of Engineering, UK
t.l.karavsilis@warwick.ac.uk; v.kamperidis@warwick.ac.uk
[c] University of New South Wales, Centre for Infrastructure Engineering and Safety, Australia
b.uy@unsw.edu.au

KEYWORDS: Fracture prediction models; finite element analysis; void growth model; cyclic loading.

INTRODUCTION

Steel cylindrical pins with hourglass-shape bending parts (called web hourglass pins – WHPs) have been recently used by the authors ([1]) as the energy dissipation system of a steel post-tensioned (PT) beam-column connection for self-centering moment-resisting frames (SC-MRFs). Pilot tests on WHPs showed their superior energy dissipation and fracture capacity [1]. However, more work is needed to assess the hysteretic behavior and low-cycle fatigue performance of WHPs for high performance steel materials such as high strength steel (HSS) and stainless steel (SS). There is limited experience on the low-cycle fatigue and fracture capacity of SS for seismic applications. SS grades are divided into three categories: austenitic, ferritic, and duplex. Austenitic is the most common type of SS. Duplex SS (referred to herein as SSD) is at least twice stronger than the common austenitic grades and highly resistant to corrosion cracking.

This paper presents the application of two micromechanics-based models for ductile fracture prediction in metals, i.e. the Void Growth Model (VGM) and the Stress Modified Critical Strain Model (SMCS). First, the critical parameters of the two models are identified using tensile tests on circumferentially-notched specimens (CNS) and complementary numerical analysis based on the finite element method (FEM). The critical parameters of the VGM and SMCS are then used to predict fracture in WHPs made of HSS grade M1020, SS grade 304 (SS304), and SSD. The FEM model shown in *Fig. 1a* was used for the numerical simulations. Fig. 1b shows that the agreement between the Fem model and the tests is good for monotonic and cyclic loading. The ability of the cyclic VGM (or CVGM) to predict ductile fracture under cyclic loading conditions is evaluated using the results of several cyclic tests on WHPs made of HSS and SS304.

CONCLUSIONS

- The void growth model (VGM) and the stress-modified critical strain (SMCS) model used to predict fracture in metals were calibrated for the HSS, SS and SSD and their parameters (critical void growth index VGI_{cr} and toughness index α) are provided. The values of these parameters are consistent with the ductility of the materials.
- Application of the VGM to the monotonic tests of the WHPs resulted in VGI values considerably lower than the VGI_{cr} at the critical locations, confirming the very low likelihood of fracture under monotonic loading. Axial restraint imposed on WHPs changes the critical location of potential fracture.
- Application of the cyclic VGM, with λ (rate of degradation of the monotonic VGI_{cr}) values taken from literature, to four cyclic WHP tests predicted fracture at a different location than that observed in the tests. Possible reasons for this discrepancy were discussed.

- WHPs made of HSS, SS and SSD are reliable devices that can be safely used as seismic energy-dissipative fuses in beam-column connections and braces with the goal of realizing a very easy-to-repair structural design concept.
- Based on this study, it is concluded that WHPs made of HSS, SS and SSD are reliable devices that can be safely used as seismic energy-dissipative fuses in beam-column connections and braces with the goal of realizing a very easy-to-repair structural design concept.

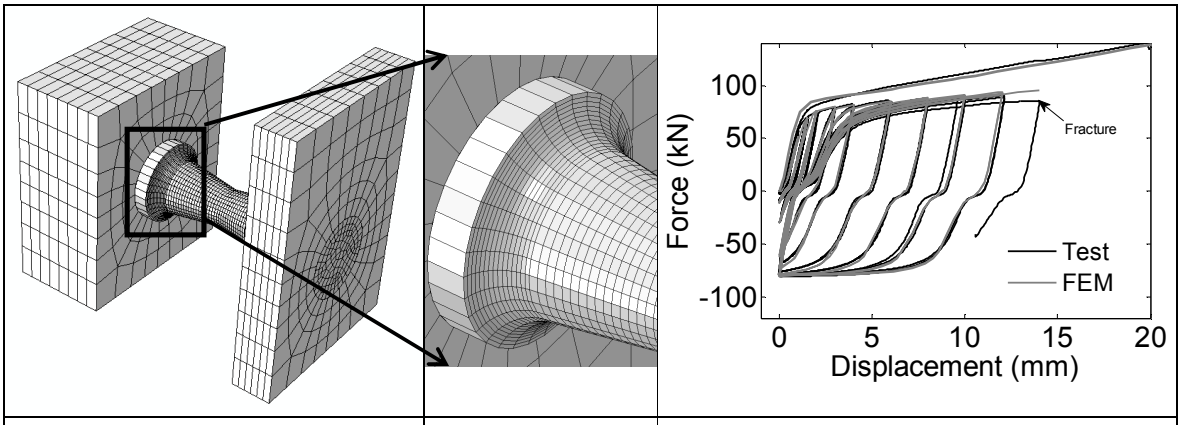

Fig. 1. a) WHP FEM model; b) mesh refinement; and c) experimental – FEM comparison for the HSS-WHP1 under the AISC loading protocol.

REFERENCES

[1] Vasdravellis, G., Karavasilis, T.L., and Uy, B. (2013a). "Large-scale experimental validation of steel post-tensioned connections with web hourglass pins". J. Struct. Eng. 139(6), 1033-1042.

[2] Hancock, J. W., Mackenzie, A. C. (1976). "On the mechanics of ductile failure in high-strength steel subjected to multi-axial stress states." J. Mech. Phys. Solids, 24(3), 147–169.

[3] Panontin, T. L., and Sheppard, S. D. (1995). "The relationship between constraint and ductile fracture initiation as defined by micromechanical analyses." *Fracture mechanics: 26th Volume*, *ASTM STP 1256*, ASTM, West Conshohoken, Pa., 54–85.

[4] Rice, J.R. and Tracey, D.M. (1969). "On the ductile enlargement of voids in triaxial stress fields". *J. Mech. Phys. Solids*, 17(3), 201-217.

[5] Kanvinde, A. M., and Deierlein, G. G. (2006). "The void growth model and the stress modified critical strain model to predict ductile fracture in structural steels." J. Struct. Eng., 132(12), 1907-1918.

[6] Abaqus user's manual

[7] Vasdravellis G., Karavasilis T.L.,Uy B. (2014). "Design rules, experimental evaluation and fracture models of high-strength and stainless-steel hourglass shape energy dissipation devices". Journal of Structural Engineering (ASCE). Accepted – in press

[8] Kanvinde, A. M., and Deierlein, G. G. (2007). "Cyclic void growth model to assess ductile fracture initiation in structural steels due to ultra-low cycle fatigue." J. Eng Mech., 133(6), 701-712.